Three-dimensional repositioning of jaw in the orthognathic surgery using the binocular stereo vision

Ismail Taha COMLEKCILER[a,*], Salih GUNES[b], Celal IRGIN[c]

[a] Department of Electrical and Electronics Engineering, Faculty of Engineering, Mevlana University, 42003, Konya, Turkey

[b] Department of Electrical and Electronics Engineering, Faculty of Engineering, Selcuk University, 42075, Konya, Turkey

[c] Department of Orthodontics, Faculty of Dentistry, Abant Izzet Baysal University, 14280, Bolu, Turkey

Abstract

In recent years, the binocular stereo vision has become more popular in many different areas because of the latest developments in three-dimensional (3-D) image processing technology that ensures rich information in comparison with other sensor types. This study presents a novel method based on the binocular stereo vision system to reduce the measurement error encountered frequently in the orthognathic surgery. The main aim is to enhance the level of the accuracy of this sensitive operation. The developed system is not only useful for the preoperative assessment or the postoperative process but also can be utilized during the real-time operation. Additionally, this system provides a broader working field, more practical and healthier environment and less expensive setup. Therefore, the developed binocular stereo vision system may be acceptable for most surgeons. Experimental results show that the average error rate for all of X, Y and Z coordinates in the Cartesian system is 0.25 mm which is clinically acceptable (< 1.00 mm). The binocular stereo vision system would be a helpful

[*] *Corresponding author:* tcomlekciler@mevlana.edu.tr (Ismail Taha Comlekciler), +90.535.569 52 43
E-mail addresses: sgunes@selcuk.edu.tr (Salih Gunes), celal.irgin@ibu.edu.tr (Celal Irgin)

throughout the orthognathic surgery to improve precision of the measurement and satisfy the healthy surgical operating environment.

Key Words: Measurement error, 3-D coordinate measurement, three-dimensional (3-D) image processing, stereo vision, stereo imaging, 3-D image-guided orthognathic surgery, real-time surgical navigation.

1. Introduction

The orthodontics is one of the oldest divisions of the dentistry. The orthognathic surgery is the surgical correction of skeletal anomalies or malformations including the maxilla or the mandible [1]. The success of the surgery depends on the correct diagnosis, and the special preoperative plan [2]. The orthognathic surgical planning should be performed correctly before the operation. According to this planning, it is necessary to reposition the jaws accurately with the desired direction and displacement, since it is crucial to re-establish physiological functions and esthetic anatomy after the surgical operation [3]. However, the orthognathic surgery studies show that there are some significant differences between the preoperative surgical planning and postoperative results [4]. These differences result from inability to transfer the numerical data, which is derived from the surgical planning to the operation accurately. This situation affects the achievement of the orthognathic surgery negatively. The major errors can be classified as application error, human error, registration error, technical error, and imaging error [5]. The mistakes that are made during the operation affect the surgery result negatively because the surgeons who are aware of these disadvantages have no intention to use the technical devices routinely. At present, the typical method for repositioning jaws in the correct location is based on the utilizing the surgical splints.

The three-dimensional (3-D) measurement of the jaw and teeth is an important task for the computerized vision systems. The stereo vision has become more popular in many different areas because of the latest development in three-dimensional technology and also vision sensors ensure rich information in comparison with other sensor types [6, 7]. Recent advances in computer vision make it possible to acquire high-resolution 3-D models of scenes and objects [8]. The advantage of 3-D model construction from two-dimensional (2-D) images is that it does not require specialized equipment; only a simple digital camera can fulfill the requirement. Specialized equipment like laser scanners can lead to a very accurate construction of 3-D models. However, this equipment is generally very expensive, and it may not be safe using in applications like human body modeling [9]. The traditional methods of preoperative preparation are based on the lateral and the frontal radiographic images and computer-based tomography devices [10–12]. Nevertheless, these devices have some significant disadvantages such as radiation, high cost, impracticality and low precision level. Therefore, numerous approaches presented in the literature in order to mitigate side effects of using such devices [13].

In this paper, a novel method is developed with 3-D image-guided surgery navigation by applying the stereo vision, in order to realize the real-time tracking the position and the rotation of the patient with the instruments. The proposed method guides the surgeon during the surgical operation whether the actual 3-D position of the jaw matches with the preoperative measurements by getting real-time, more accurate information of repositioning of the irregular jaw sections.

The rest of paper starts with introducing stereo processing in Section 2. The experimental setup and measurements are given in Section 3. Section 4 discusses and analyzes the experimental results. Section 5 concludes the paper.

2. Stereo Processing

The system consists of pre-calibrated binocular stereo camera operating in the visible spectrum and software. Algorithms have been developed in order to register 3-D depth information for the stereoscopic images and estimate some reposition values from them. A user graphical interface is developed as a practical tool to select the desired points and to display the results.

The stereo processing is implemented by three main steps [14]:

i. Identify correlation between image features in different views of the scene,
ii. Compute the relative changes between pointed coordinates in each image,
iii. By applying the camera geometry, specify the 3-D position of the points relative to the camera.

2.1. Image Acquisition

The image acquisition, defined as retrieving an image from a hardware-based source such as camera, is always the first step in the image processing. The pre-calibrated binocular camera (BumbleBee2 - Point Grey Research, Inc.) is used which is aligned in parallel (with a fixed position) with the baseline of 120 mm and 1032 × 776 maximum pixels. It has a 6-pin IEEE-1394a OHCI PCI Host Adapter for camera control and video data transmission. In order to process the acquired images, a specialized software is developed using Birchfield and Tomasi’s pixel by pixel stereo matching algorithm [15].

2.2. Disparity Maps

The two image-sensors (cameras) of the binocular stereo vision system reside on the different horizontal coordinates along the same line. Thus, any point in the 3-D projection maps to the two different locations on the image-sensors. The difference between the coordinates of the same features on the left and right image (Figure 1) will define the disparity for the any point of the image $d(P)$. The computation is done by the following steps:

Disparity for the feature A is defined as $d(A) = X(A_{left}) - X(A_{right})$ and the disparity of point B will be derived as $d(B) = X(B_{left}) - X(B_{right})$ where $X(A_{left})$ is the X coordinate of the point A_{left} [14].

The images captured from the two horizontally displaced camera positions produce different perspectives of the same scene, which helps in calculating the difference in relative displacement of the objects in the scene. This relative displacement is referred to as disparity [16]. The computation of the disparity map as shown in Figure 2a is a key step to obtain the depth information in the form of a 3-D depth map as shown in Figure 2b. The Sum of Absolute Differences Correlation method of stereo vision is used to calculate disparity (1).

The approach is led by following processes:

i. Fetch a pixel from the right image,
ii. From the left image find a neighborhood of the given right image,
iii. Compare this neighborhood to a number of neighborhoods along the same row,
iv. Choose the best match for disparity map.

According to the following (1) the comparisons of neighborhoods or masks are computed [14]:

$$min_{d=d_{min}}^{d_{max}} \left(\sum_{i=-\frac{m}{2}}^{\frac{m}{2}} \left(\sum_{j=-\frac{m}{2}}^{\frac{m}{2}} \left(\left| \mathrm{I}_{right}[x+i][y+j] - \mathrm{I}_{left}[x+i+d][y+j] \right| \right) \right) \right) \tag{1}$$

where d_{min} and d_{max} are the minimum and the maximum disparities of d, m is the mask size, I_{right} and I_{left} are the right and left images, x and y are the points' coordinates in images [15].

2.3. The Computation of the 3-D Coordinates

In this study, the 3-D depth information about the object is constructed via the stereo triangulation principle which is based on the difference of an object's location in two images because of the changed view of the perspective. One of the key elements in 3-D algorithms is to convert image values (in the pixel space) into the real world Cartesian coordinates, accurately (Figure 3) [6].

The triangulation formulation is based on the similarity between the triangles as seen from (2), for which all the ratios

$$\frac{B}{Z} = \frac{B-(X^l - X^r)}{Z-f} = \frac{X^l - X^r}{f} = \frac{d}{f} \tag{2}$$

are equal.

This leads to the following formulation to calculate the distance Z, where d ($d = X^l - X^r$) is the disparity, f is the focal length, B is the baseline, X^l is the column position information on the left image of the measured object P as shown in Figure 3a. Similarly, X^r is the column position information on the right image of the measured object P. Once the image of the 3-D depth map is obtained, the depth measurements are carried out as seen from the following (3);

$$\frac{B}{Z} = \frac{d}{f} \rightarrow Z = f\frac{B}{d} \tag{3}$$

The baseline B is defined as the distance between the two camera centers. The focal length f is predefined by the employed camera. The accuracy of the system increases with increasing the baseline (B) due to the limitations on the camera resolution for a fixed distance [17]. Figure 3b shows the relationship between the distance and the disparity.

After Z is determined, X and Y can be calculated using the usual projective camera by the (4) and (5):

$$\mathrm{X} = u\frac{Z}{f} \tag{4}$$

$$\mathrm{Y} = v\frac{Z}{f} \tag{5}$$

where u and v are the pixel location in the 2-D image. X, Y and Z values are the real 3-D positions.

Finally, a complete image of real 3-D depth map (Figure 2b) can be constructed from image of the disparity map (Figure 2a). X, Y and Z movement information of final locations of upper and lower jaws is reported to the surgeon through a developed user interface software.

3. Experimental Setup and Measurements

This part, first, explains the preparation of the dental plaster model and continues with the image rotation, segmentation and ends with the distance calculation. Figure 4 shows the articulator (SAM 3 made by SAM Präzisionstechnik GmbH) used in this study that has similar functionality to caliper and is utilized to calculate the movement by transferring the position of the patient’s jaw, teeth and the face in a 3-D space.

3.1. The Dental Plaster Model

In the orthognathic surgery, preliminary surgical plans are designed through building the jaw models from the molded dental plasters of the upper and the lower teeth. The performance of the developed binocular stereo vision system in this study, will be compared to the conventional dental plaster models to prove the new concept.

As shown in Figure 5a, first of all, the patients` lower and upper jaw plaster models are manufactured by using a device called articulator. Before the operation, the position of upper and lower-jaw-teeth of the patient is closed. Then, the positioning of teeth of the closed jaws are marked in red ink by the dental surgeon. Similarly, the expected closed teeth positions after the correction operation are marked. Finally, the difference between the positions is determined in mm. These positions are shown in Figure 5b and Figure 5c. To improve the results, measurements are realized three times for each closed positions of the teeth before and after operation. Eventually, the final value that will be considered in the operation is based on the average of three independent measurements.

The X, Y, Z positions of all the marked teeth (Figure 6) of the patient`s upper and lower jaws are measured manually with a mechanical compass by the dental surgeon (Figure 7a). For this particular patient, there are 14 teeth at lower jaw and 12 at the upper jaw. All of these 26 teeth`s Cartesian coordinate values are measured and recorded with respect to a reference point. Similarly, the same measurements are carried out by the developed binocular stereo vision system (Figure 7b).

The measurement results are obtained by using the difference between the initial and the final positions of the jaws for the calculation of the displacements of the jaws in the

Cartesian coordinates. Finally, the measurement error is calculated by comparing the conventional manual system with the developed binocular stereo vision system.

3.2. Image Rotation

During the experimental studies, it has been noticed that the apparatus and the camera could not be kept the original angular position of their locations. For this reason, some rotations are observed in the X-Y directions. To prevent the error due to the post-operation image is rotated in the theta (θ) amount and it is matched with the pre-operation image (Figure 8).

In order to compute a rotation by using matrices, the point (x, y) in two dimensions, (orientation from positive x to y) is written as a vector and then multiplied by a rotation matrix from the angle θ (theta) (6) and (7):

$$R(\theta) = \begin{bmatrix} cos\theta & -sin\theta \\ sin\theta & cos\theta \end{bmatrix} \tag{6}$$

$$\begin{bmatrix} x' \\ y' \end{bmatrix} = \begin{bmatrix} cos\theta & -sin\theta \\ sin\theta & cos\theta \end{bmatrix} . \begin{bmatrix} x \\ y \end{bmatrix} \tag{7}$$

where (x', y') are the coordinates of the point after the rotation. The formulation for x' and y' can be seen in (8) and (9) [18];

$$x' = x.cos\theta - y.sin\theta \tag{8}$$

$$y' = x.sin\theta + y.cos\theta \tag{9}$$

3.3. Segmentation

A fundamental operation in digital image processing is color image segmentation with many variants presented in the literature [19]. In this section, prior to segmentation, surgeon marks a point on the image. To confirm the stereo vision system's results, the average value of three manual measurements of the marked points on the teeth are used. The X, Y, Z positions of the marked points are manually measured with a mechanical compass (caliper) with respect to a reference point. This operation is repeated three times to minimize measurement errors. In question selected points are approximately marked on the image as well. There may be some shifts on the image due to the manual selection of these points in the image which has a low resolution due to zoom effect.

First of all, to eliminate these errors and to identify these points accurately, the marked area is segmented using a threshold value and the R-G-B (Red- Green- Blue) values of the neighboring points in the 9 × 9 matrix. If the any one of the R-G-B values of the examining point is out of range then this point is eliminated and it is not included in the segmented area. Secondly, after the area segmentation, the geometric center of this shape is assigned as the marked point for each one of XY, XZ and YZ-plane. In this way, it is determined with a high precision (Figure 9).

3.4. Distance Calculation

The distances of the new position of the jaws are calculated by obtaining pre-assigned measurement points (Figure 6) on the pre-operation and the post-operation images. The positional changes in (X, Y, Z) coordinate values of the marked point can be formulated in the following (10) – (12):

$$Movement(X) = \left| PostOperation(X) - PreOperation(X) \right| \tag{10}$$

$$Movement(Y) = \left| PostOperation(Y) - PreOperation(Y) \right| \tag{11}$$

$$Movement(Z) = \left| PostOperation(Z) - PreOperation(Z) \right| \tag{12}$$

The next section will provide experimental and statistical results.

4. Experimental Results and Analysis

The application does not regard solely the scanning of plaster models, but also for the real time navigation of the patient. The purpose of using plaster models in this study is to verify the effectiveness of the proposed method. Thus once it is verified, the model will also be used in applications like human body. In this study, the stereo camera is used to take "one single shot" (one stereo pair) of part of teeth and to convert it to 3-D image. As the image from this viewpoint provides sufficient information to make the necessary measurements to locate the teeth, a fully 3-D reconstruction process is not needed. In addition, quality inspection process is sufficient to measure and locate the teeth from a partly constructed 3-D image.

To calculate the approximation error along the (X, Y, Z) coordinates in millimeters (mm), a movable lower and upper plaster models of jaw of the patient for experiments are built as shown in Figure 5. The error values are calculated as absolute difference of accurate measurement values of caliper (manual) and stereo vision system reposition values ($\left|Manual - Stereo\ Vision\right|$).

The coordinate changes of the selected points and the error rates for X, Y and Z axes are given in Table 1, Table 2 and Table 3, respectively. The measurement errors for the upper and the lower jaws are provided separately in the given tables. The tooth numbers are given for the right and the left side of each jaw. The layout of teeth in a jaw is given in Figure 6. As the acceptable error should be lower than 1 mm, the measurements clearly suggests the success of the proposed method.

The mean error rates for X, Y and Z coordinates are 0.25 mm, 0.26 mm and 0.25 mm, respectively. The standard deviation rates for X, Y and Z coordinates are 0.18, 0.19 and 0.17, respectively. The experimental measurements for X, Y and Z statistically lead to results of 0.25 ± 0.18 mm, 0.26 ± 0.19 mm and 0.25 ± 0.17 mm, respectively. As it is clearly seen, they are clinically acceptable values (< 1.00 mm) [20].

As the acceptable error should be lower than 1.00 mm and dispersion of the measurement errors do not exceed the target value, the measurements clearly suggest the success of the stereo vision system. The reasons for the inhomogeneous distribution of errors may be accumulating from improper lux level of the illumination [14] on the object and the camera or the user`s carelessness on the activation operation or the miscalculation distances of 3-D images.

In order to further explain the results, the comparisons between the manual measurements and the stereo vision measurements are illustrated in Figure 10. The correlation diagrams show the measurement differences with respect to the 45º diagonal for each axis. The measurement points along the 45º diagonal show the correct measurements. The divergence in the line is caused by the measurement error between the manual and the stereo vision measurement values.

In this research study, the Statistical Package for Social Sciences (SPSS) version 21.0 is used for the Cronbach's alpha reliability analysis of the measurements. The Cronbach's alpha (α) reliability analysis [21] is used to measure the consistency level statistically. Table 4 shows the consistency level of a measurement. Higher alpha values indicate that measurements are acceptable whereas lower alpha values indicate that measurements are unacceptable (α < 0.5). The results of analysis are summarized in Table 5. As observed from Table 4 and Table 5; all alpha values are greater than 0.9 with highest level of consistency.

5. Conclusion

This paper focuses on the reduction of measurement errors of the orthognathic surgery based on the binocular stereo vision. As a case study, the proposed method applied to be used by dental surgeons. The proposed method improves the precision by using the binocular stereo vision technology and satisfies the surgical operation environment in the range of 600 – 750 mm. The results show a high positioning accuracy of measurements between the post-operation and the pre-operation measurement points. Cronbach's alpha reliability results are all favorable. Finally, the results in 3-D depth measurements show that binocular stereo vision can be reliably used to reduce measurements error as an alternative method in the orthognathic surgery. As a future study, 3-D printed and coordinate measurement machine (CMM) models would be applied to verify the correctness and efficiency of the proposed method. Furthermore, as the accuracy is the main concern of this case study, recently developed stereo vision algorithms would be applied in order to obtain better measurements. The ultimate purpose of this study is in-vivo binocular stereo vision measurement to be used in surgical operational environment. Nevertheless, there are some difficulties to be addressed such as the proper determination of measurement location points including reference point on real jaws and positioning of binocular stereo cameras across patient's face to measure the precise displacement of jaw(s). In addition, the artificial intelligence methods has great potential to improve the accuracy of measurements and the capability of instrumentation in many application areas [22]. It is considered that the proposed approach can be enhanced with artificial intelligence techniques.

Acknowledgment

This study is supported by Selcuk University (Project No: 12201010). The author appreciates the BAP Office (Scientific Research Projects Coordination Unit) of Selcuk University for generously funding this scientific research project. The special thanks to the academic staff of the Department of Orthodontics in Abant Izzet Baysal University.

References

[1] Yanping, L., Dedong, Y., Xiaojun, C., Xudong, W., Guofang, S. and Chengtao, W. "Simulation and evaluation of a bone sawing procedure for orthognathic surgery based on an experimental force model", *J. Biomech. Eng.*, **136**(3), pp. 1–7, (2014).

[2] Janssen, R., Lou, E., Durdle, N.G., Raso, J., Hill, D., Liggins, A.B. and Mahood, S. "Active markers in operative motion analysis", *IEEE Transactions on Instrumentation and Measurement*, **55**(3), pp. 854–859, (2006).

[3] Chapuis, J., Schramm, A., Pappas, I., Hallermann, W., Schwenzer-Zimmerer, K., Langlotz, F. and Caversaccio, M. "A new system for computer-aided preoperative planning and intraoperative navigation during corrective jaw surgery", *IEEE Transactions on Information Technology in Biomedicine*, **11**(3), pp. 274–287, (2007).

[4] Bell, R.B. "Computer planning and intraoperative navigation in orthognathic surgery", *J. Oral Maxillofac. Surg.*, **69**(3), pp. 592–605, (2011).

[5] Widmann, G., Stoffner, R. and Bale, R. "Errors and error management in image-guided craniomaxillofacial surgery", *Oral Surg. Oral Med. Oral Pathol. Oral Radiol. Endod.*, **107**(5), pp. 701–715, (2009).

[6] Anchini, R., Liguori, C., Paciello, V. and Paolillo, A. "A comparison between stereo-vision techniques for the reconstruction of 3-d coordinates of objects", *IEEE Transactions on Instrumentation and Measurement*, **55**(5), pp. 1459–1466, (2006).

[7] Pachidis, T.P. and Lygouras, J.N. “Pseudostereo-vision system: a monocular stereo-vision system as a sensor for real-time robot applications”, *IEEE Transactions on Instrumentation and Measurement*, **56**(6), pp. 2547–2560, (2007).

[8] Tosca, A., Kokolakis, A., Lasithiotakis, K., Zacharopoulos, A., Zabulis, X., Marnelakis, I., Ripoll, J. and Stephanidis, C. “Development of a three-dimensional surface imaging system for melanocytic skin lesion evaluation”, *J. Biomed. Opt.*, **18**(1), pp. 1–12, (2013).

[9] Jain, A., Yadav, V., Mittal, A. and Gupta, S. “Probabilistic approach to modeling of 3d objects using silhouettes”, *J. Comput. Inf. Sci. Eng.*, **6**(4), pp. 381–389, (2006).

[10] Tognola, G., Parazzini, M., Pedretti, G., Ravazzani, P., Svelto, C., Norgi, M. and Grandori, F. “Three-dimensional reconstruction and image processing in mandibular distraction planning”, *IEEE Transactions on Instrumentation and Measurement*, **55**(6), pp. 1959–1964, (2006).

[11] Tsuji, M., Noguchi, N., Shigematsu, M., Yamashita, Y., Ihara, K., Shikimori, M. and Goto, M. “A new navigation system based on cephalograms and dental casts for oral and maxillofacial surgery”, *Int. J. Oral Maxillofac. Surg.*, **35**(9), pp. 828–836, (2006).

[12] Birkfeller, W., Huber, K., Larson, A., Hanson, D., Diemling, M., Homolka, P. and Bergmann, H. “A modular software system for computer-aided surgery and its first application in oral implantology”, *IEEE Trans. Med. Imaging*, **19**(6), pp. 616–620, (2000).

[13] Bhowmik, U.K. and Adhami, R.R. “A novel technique for mitigating motion artifacts in 3D brain imaging systems”, *Scientia Iranica*, **20**(3), pp. 746–759, (2013).

[14] Comlekciler, I.T., Gunes, S., Irgin, C. and Karlik, B. "Measuring the optimum lux value for more accurate measurement of stereo vision systems in operating room of orthognathic surgery", *IEEE 11th International Conference on Electronics Computer and Computation (ICECCO '14)*, Abuja, Nigeria, pp. 1–6 (2014).

[15] Birchfield, S. and Tomasi, C. "Depth discontinuities by pixel-to-pixel stereo", *IEEE Sixth International Conference Computer Vision*, Bombay, India, pp. 1073–1080 (1998).

[16] Muthukkumar, S.K. and Oliver, J.H. "Sensor augmented virtual reality based teleoperation using mixed autonomy", *J. Comput. Inf. Sci. Eng.*, **9**(1), pp. 1–5, (2009).

[17] Chu, J., Jiao, C., Guo, H. and Zhang, X. "Binocular stereo vision system design for lunar rover", *SPIE Pattern Recognition and Computer Vision (MIPPR 2007)*, 6788, Wuhan, China, pp. 1–8 (2007).

[18] Lounesto, P. "Clifford algebras and spinors", In *London Mathematical Society Lecture Note Series*, 2nd Edn., Cambridge University Press, London, UK, (2001).

[19] Abadpour, A. and Kasaei, S. "Principal color and its application to color image segmentation", *Scientia Iranica*, **15**(2), pp. 238–245, (2008).

[20] Li, B., Zhang, L., Sun, H., Shen, S.G. and Wang, X. "A new method of surgical navigation for orthognathic surgery: optical tracking guided free-hand repositioning of the maxillomandibular complex", *J. Craniofac. Surg.*, **25**(2), pp. 406–411, (2014).

[21] Cronbach, L.J. "Coefficient alpha and the internal structure of tests", *Psychometrika*, **16**(3), pp. 297–334, (1951).

[22] Alippi, C., Ferrero, A. and Piuri, V. "Artificial intelligence for instruments and measurement applications", *IEEE Instrumentation & Measurement Magazine*, **1**(2), pp. 9–17, (1998).

1

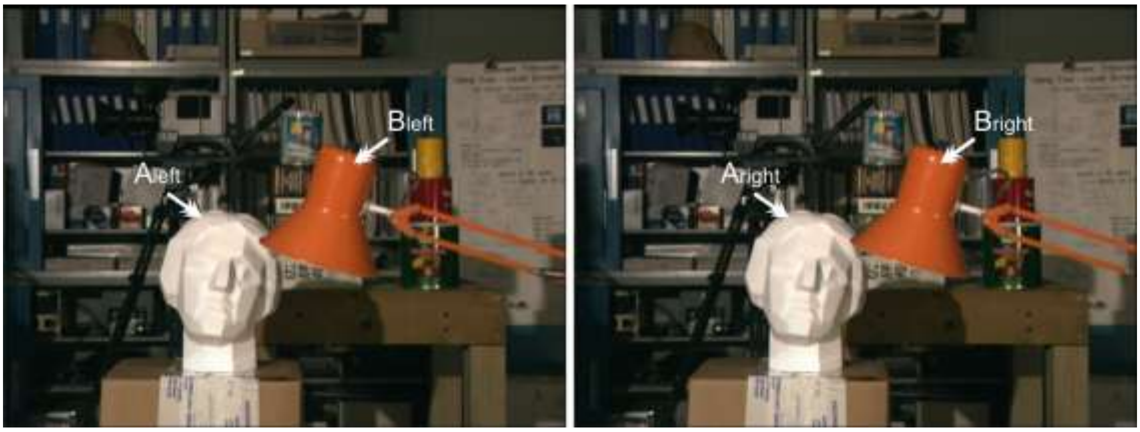

Figure 1. Example of matching points between stereo vision images. The Tsukuba image is taken from Middlebury Stereo Evaluation (http://vision.middlebury.edu/stereo)

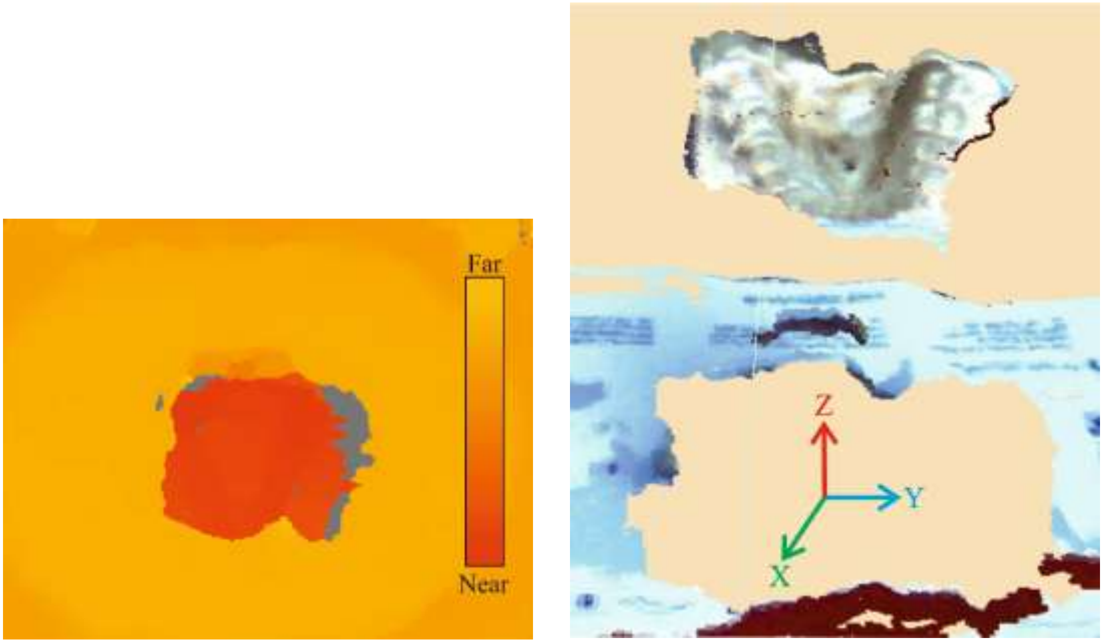

(a) (b)

Figure 2. Main stages for the depth measurement process: (a) image of disparity map (b) image of 3-D depth map.

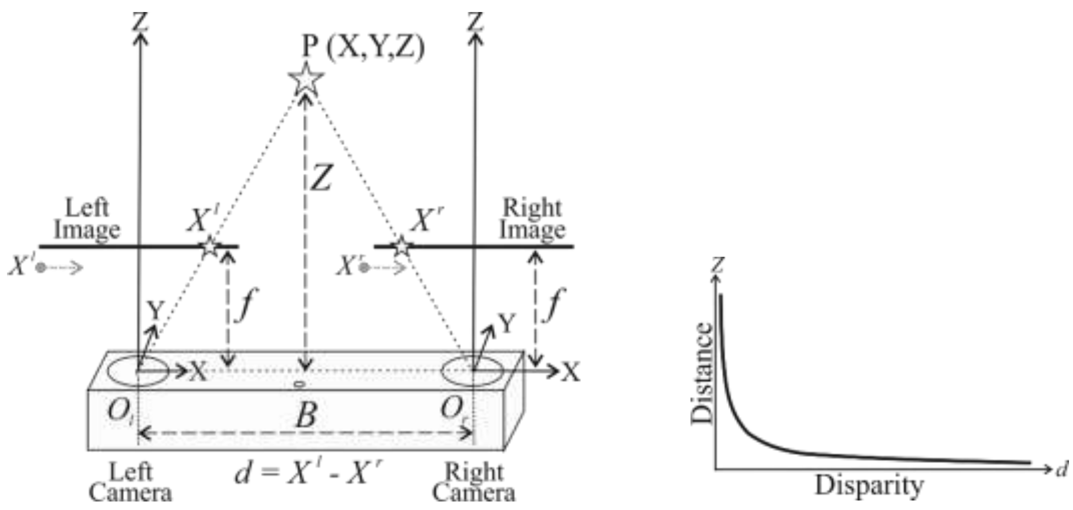

(a) (b)

Figure 3. (a) Basic diagram of a binocular stereo vision system (b) distance versus disparity relationship [6, 7].

Figure 4. A 3-D dental plaster jaw model installed into an articulator for surgical planning and simulation.

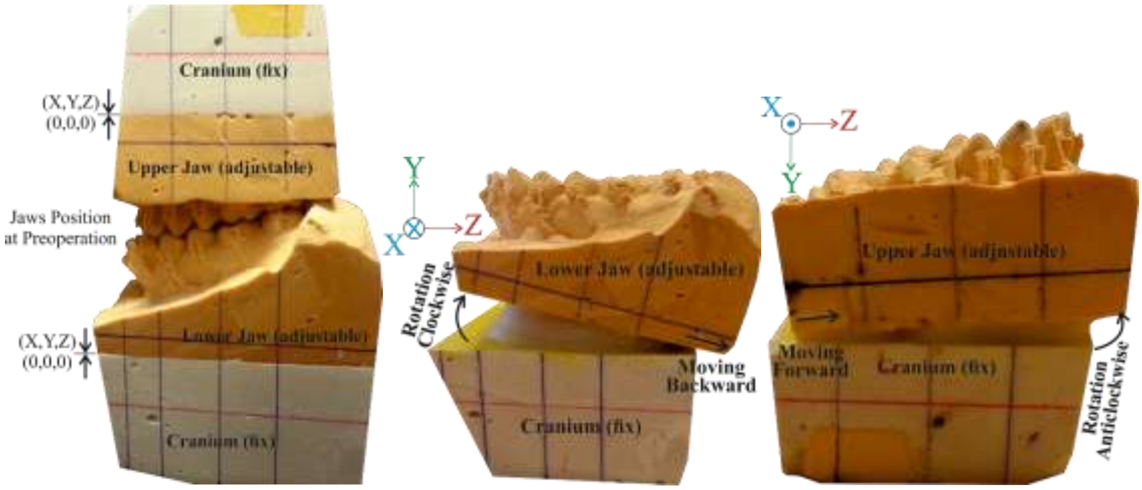

(a) (b) (c)

Figure 5. (a) Pre-operation dental plaster model (b) post-operation lower jaw positioned to rotation clockwise and moving backward (mandibula) (c) post-operation upper jaw model positioned to rotation anticlockwise and moving forward (maxilla).

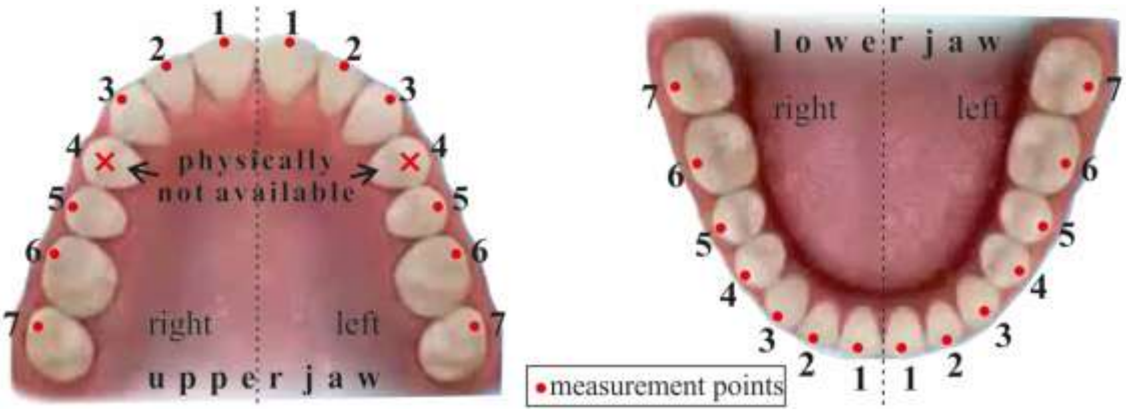

Figure 6. Upper and lower jaw measurement location points.

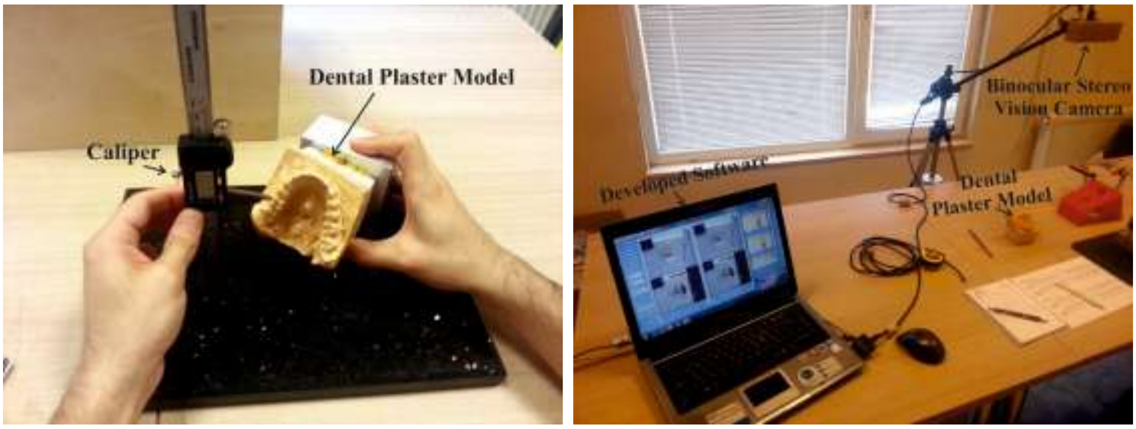

(a) (b)

Figure 7. (a) Manual and (b) stereo vision measurements.

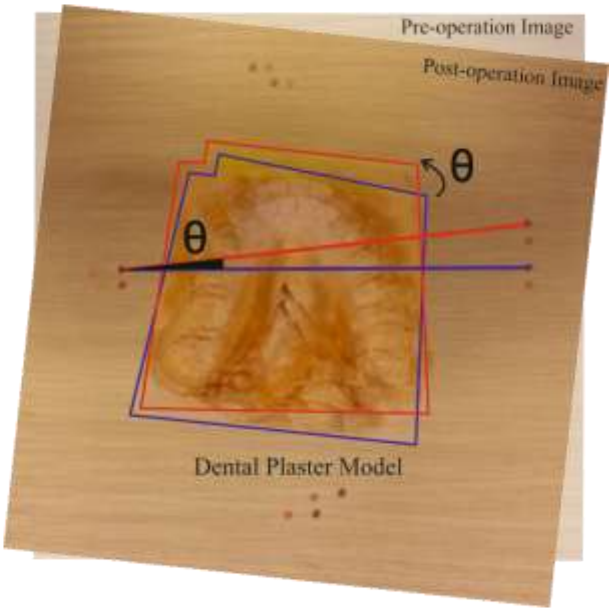

Figure 8. Dental plaster model image rotation.

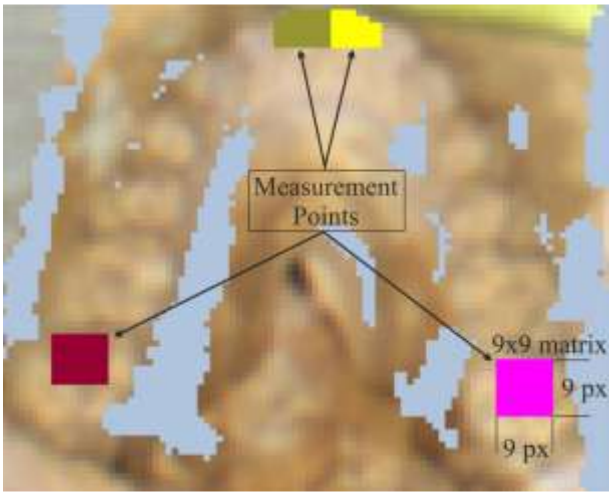

Figure 9. Segmentation.

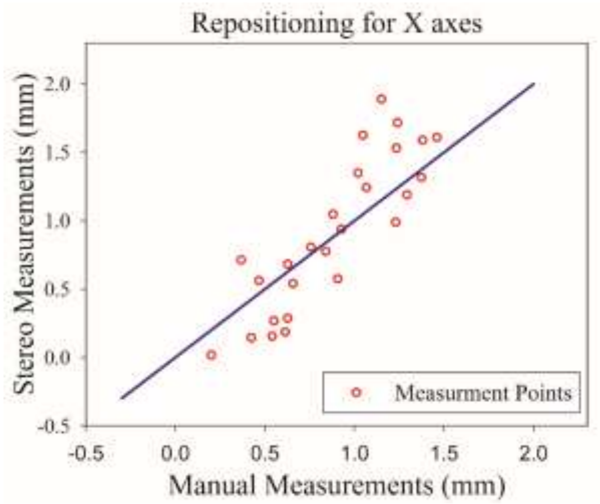

(a)

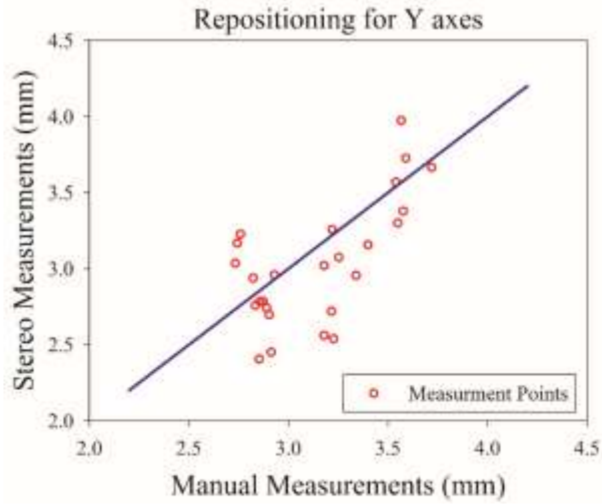

(b)

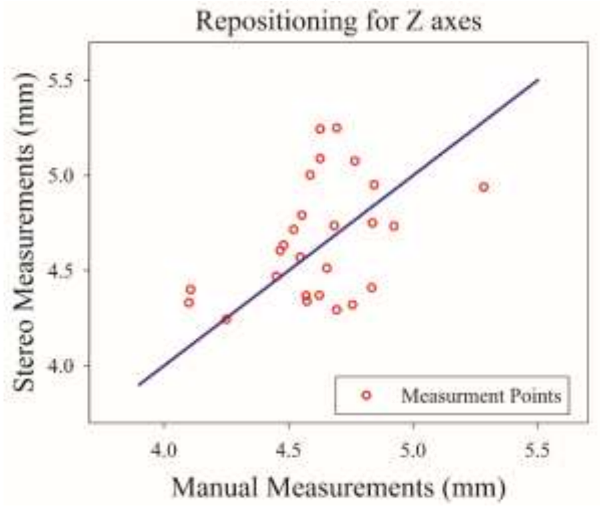

(c)

Figure 10. Stereo measurements compared to manual measurements for the repositioning of (a) X, (b) Y and (c) Z axes.

Table 1. Repositioning experimental results for X axes (transversal) coordinates

Exp.		Upper Jaw														Mean Err.	σ
		Right							Left								
	Tooth No	7	6	5	4*	3	2	1	1	2	3	4*	5	6	7		
X	Man.	0.93	0.63	0.91		0.37	0.66	0.20	0.42	0.54	0.61		0.47	0.55	0.63		
X	Str. Vis.	0.94	0.68	0.58		0.71	0.54	0.02	0.14	0.16	0.19		0.56	0.27	0.29		
X	Err.	0.01	0.05	0.33		0.34	0.12	0.18	0.28	0.39	0.42		0.09	0.28	0.34		
Exp.		Lower Jaw														0.25	0.18
		Right							Left								
	Tooth No	7	6	5	4	3	2	1	1	2	3	4	5	6	7		
X	Man.	1.37	1.29	0.88	1.23	1.38	0.84	1.23	1.46	1.05	1.24	1.15	1.07	1.02	0.76		
X	Str. Vis.	1.32	1.19	1.05	0.99	1.59	0.78	1.53	1.61	1.63	1.72	1.89	1.24	1.35	0.81		
X	Err.	0.05	0.10	0.17	0.24	0.21	0.06	0.30	0.15	0.58	0.48	0.74	0.17	0.33	0.05		

* = Physically not available, σ = Standard Deviation, Unit = millimeter (mm),
Man. = Manual, Str. Vis. = Stereo Vision, Err. = Error, Exp. = Experiments.

Table 2. Repositioning experimental results for Y axes (vertical) coordinates

	Exp.	Upper Jaw														Mean Err.	σ
		Right							Left								
	Tooth No	**7**	**6**	**5**	**4***	**3**	**2**	**1**	**1**	**2**	**3**	**4***	**5**	**6**	**7**		
Y	**Man.**	2.93	2.87	2.91		2.82	2.85	2.73	2.76	2.74	2.83		2.89	2.86	2.90		
	Str. Vis.	2.96	2.79	2.45		2.94	2.41	3.04	3.23	3.17	2.76		2.74	2.78	2.70		
	Err.	0.03	0.08	0.46		0.12	0.44	0.31	0.47	0.43	0.07		0.15	0.08	0.20		
	Exp.	**Lower Jaw**														0.26	0.19
		Right							**Left**								
	Tooth No	**7**	**6**	**5**	**4**	**3**	**2**	**1**	**1**	**2**	**3**	**4**	**5**	**6**	**7**		
Y	**Man.**	3.59	3.57	3.55	3.34	3.25	3.23	3.22	3.18	3.18	3.22	3.40	3.54	3.58	3.72		
	Str. Vis.	3.73	3.98	3.30	2.96	3.08	2.54	2.72	3.02	2.56	3.26	3.16	3.57	3.38	3.67		
	Err.	0.14	0.41	0.25	0.38	0.17	0.69	0.50	0.16	0.62	0.04	0.24	0.03	0.20	0.05		

* = Physically not available, σ = Standard Deviation, Unit = millimeter (mm),
Man. = Manual, Str. Vis. = Stereo Vision, Err. = Error, Exp. = Experiments.

Table 3. Repositioning experimental results for Z axes (sagittal) coordinates

	Exp.	Right							Left							Mean Error (mm)	σ
Upper Jaw	**Tooth No**	**7**	**6**	**5**	**4***	**3**	**2**	**1**	**1**	**2**	**3**	**4***	**5**	**6**	**7**		
Z	**Man.**	4.63	4.77	4.83		4.92	4.84	5.28	4.52	4.48	4.47		4.25	4.11	4.10		
	Str. Vis.	5.24	5.08	4.41		4.73	4.75	4.94	4.72	4.63	4.61		4.24	4.40	4.33		
	Err.	0.62	0.31	0.42		0.19	0.09	0.34	0.20	0.15	0.14		0.01	0.29	0.23		
Lower Jaw	**Exp.**	**Right**							**Left**							0.25	0.17
	Tooth No	**7**	**6**	**5**	**4**	**3**	**2**	**1**	**1**	**2**	**3**	**4**	**5**	**6**	**7**		
Z	**Man.**	4.55	4.55	4.69	4.57	4.59	4.84	4.68	4.65	4.45	4.62	4.69	4.76	4.63	4.57		
	Str. Vis.	4.79	4.57	5.25	4.34	5.00	4.95	4.74	4.51	4.47	4.37	4.29	4.32	5.09	4.37		
	Err.	0.24	0.02	0.56	0.23	0.42	0.11	0.05	0.14	0.02	0.25	0.40	0.44	0.46	0.20		

* = Physically not available, σ = Standard Deviation, Unit = millimeter (mm),
Man. = Manual, Str. Vis. = Stereo Vision, Err. = Error, Exp. = Experiments.

Table 4. The consistency levels of the Cronbach's Alpha

Cronbach's Alpha	Internal Consistency
$\alpha \geq 0.9$	Excellent (High-Stakes Testing)
$0.7 \leq \alpha < 0.9$	Good (Low-Stakes Testing)
$0.6 \leq \alpha < 0.7$	Acceptable
$0.5 \leq \alpha < 0.6$	Poor
$\alpha < 0.5$	Unacceptable

Table 5. Cronbach's Alpha (α) reliability analysis results

Cronbach's Alpha (α) Reliability Analysis	Manual Measurements	Stereo Vision Measurements	Manual + Stereo Vision Measurements
X axes (Transversal)	0.976	0.979	0.977
Y axes (Vertical)	0.981	0.974	0.978
Z axes (Sagittal)	0.907	0.901	0.904

Ismail Taha Comlekciler received the B.S. degrees from Erciyes University Kayseri, M.S. degrees from Selcuk University, Konya, Turkey, in 2004 and 2009, respectively. He is currently pursuing the Ph.D. degree in Selcuk University, Konya, Turkey since August 2009. His research interests include intelligent control systems and robotics, biomedical systems, biomedical signals, image processing.

Prof. Dr. Salih Gunes received the B.S. degrees from Erciyes University Kayseri, M.S., and Ph.D. degrees from Selcuk University, Konya, Turkey, in 1989, 1993, and 2000, respectively. He is currently Prof. Dr. in the Department of Electrical-Electronics Engineering, University of Selcuk, Turkey. His research interests include artificial intelligent systems, biomedical systems, biomedical signals, image processing, circuits and systems.

Assis. Prof. Dr. Celal Irgin received the B.S., M.S., and Ph.D. degrees from Selcuk University, Konya, Turkey, in 1998, 2004 and 2010, respectively. He is currently Assis. Prof. Dr. in the Department of Orthodontics, University of Abant Izzet Baysal, Turkey. His research interests Orthodontics.